Sensory Neurons With Activated Caspase-3 Survive Long-Term Experimental Diabetes

Chu Cheng and Douglas W. Zochodne

Long-term experimental diabetes may best model the prominent and irreversible sensory deficits of chronic human diabetic polyneuropathy. Whereas irretrievable loss of sensory neurons, if present, would be an unfortunate feature of the disease, systematic unbiased counting has indicated that sensory neurons survive long-term experimental diabetes. In this study, we examined whether incipient cell loss from apoptosis in chronic experimental diabetes might nonetheless be in process, or whether neurons somehow adapt to their chronic insults. We examined sensory neurons in L4 and L5 dorsal root ganglia of long-term experimental streptozotocin-induced diabetic rats using transferase-mediated dUTP nick-end labeling (TUNEL), 4′,6-diamidino-2-phenylindole (DAPI) staining of nuclear morphology, and electron microscopic appraisal of cell morphology. None provided any evidence for ongoing apoptosis. Despite this confirmation that sensory neurons survive, neurons had elevated expression of activated caspase-3 in unique patterns that included their nuclei, cytoplasm, and proximal axonal segments. Bcl-2 expression, a marker of antiapoptosis signaling, was observed in similar numbers of diabetic and nondiabetic neurons. In contrast, diabetic sensory neurons had elevated expression of the DNA repair enzyme poly(ADP-ribose) polymerase (PARP) in their nuclei, cytoplasm, and proximal axonal segments not overlapping with caspase-3 localization. Diabetic sensory neurons also had an apparent rise in cytoplasmic labeling of nitrotyrosine, a marker of peroxynitrite toxicity reported to activate PARP. *Diabetes* 52:2363–2371, 2003

The hypothesis that caspase activation and sensory neuron apoptosis are inexorably intertwined may not always be the case. Long-term survival of sensory neurons may allow sensory deficits in diabetes to later recover. The prevalence of human diabetic sensory polyneuropathy, an intractable disorder that renders pain, sensory loss, and risks of lower-limb amputation, is increasing. How sensory deficits develop from the impact of decades of hyperglycemia is uncertain.

From the University of Calgary, Calgary, Alberta, Canada.

Address correspondence and reprint requests to Dr. D.W. Zochodne, University of Calgary, Department of Clinical Neurosciences, Room 182A, 3330 Hospital Dr., N.W., Calgary, Alberta T2N 4N1. E-mail: dzochodn@ucalgary.ca.

Received for publication 10 January 2003 and accepted in revised form 4 June 2003.

DAPI, 4′,6-diamidino-2-phenylindole; DRG, dorsal root ganglia; OCT, optimum cutting temperature; PARP, poly(ADP-ribose) polymerase; STZ, streptozotocin; TUNEL, transferase-mediated dUTP nick-end labeling.

Sensory ganglia neurons may represent an important target of diabetes by the nature of several physiological characteristics they possess (1). These include a higher requirement for local blood flow and partial autoregulation, greater metabolic demands, and a relatively leaky blood-ganglion barrier (2,3). Despite their vulnerability, we have observed evidence that such neurons may survive the ravages of diabetes. In our previous report, both rigorous whole L5 ganglion counts of neuron numbers in a 12-month diabetic model and blinded evaluation of neurons under light microscopy did not identify significant loss or degeneration in diabetes. Sensory neurons do develop atrophy and declines in their synthesis and export into axons of important structural axon proteins, such as neurofilament subunits and tubulin (4,5). Moreover, given enough time, models of experimental diabetes downregulate their expression of other important constituents, such as α- and β-calcitonin gene-related peptide, Trks A, B, and C, and pituitary adenylate cyclase-activating polypeptide. Such changes may result in "dying back" of their sensory neuron terminals and may account for the loss of terminal innervation apparent in human diabetes. Overall, the mechanisms of axon, Schwann cell, and perhaps neuron cell body damage in diabetes that have been widely considered in experimental diabetes include: *1*) excessive polyol flux associated with depletion of *myo*-inositol, accumulation of sorbitol, and heightened activation of protein kinase C subunits (6–12); *2*) direct hypoxia and ischemia of nerve trunks and ganglia (13–15); *3*) excessive oxidative stress that targets neurons, Schwann cells, and microvessels (16,17); *4*) glycosylation of structural nerve proteins (18); and *5*) deficiencies in growth factor support of neurons (19). Of these mechanisms, we propose that selective ischemia of ganglia and chronic low-grade rises in the generation of nitric oxide render nitrative stress (20–22).

A great deal of experimental diabetes work has examined relatively short-term models spanning 2–3 months. Despite their ubiquity, these models fail to reflect the chronicity of the human disease and may not portray accurate mechanisms of its impact on sensory neurons. Reports of prominent neuron apoptosis (>30%) rendering cell death after 2–3 months of experimental diabetes induced by streptozotocin in rats are unconvincing because parallel massive loss of axons in models or in humans shortly after the onset of diabetes generally does not occur (23,24). Similarly, approaches to neuron culture are complicated by the injury response of cultured neurons and the requirement of hyperglycemia to normally maintain them. Models of diabetes that are longer in

duration and reflect more gradual changes in sensory neurons may be more convincing.

In this study, we addressed whether chronic apoptotic-like morphological changes, perhaps termed "apoptosis lente," might be a feature of sensory neurons in a long-term model of experimental diabetes. If such features were present, it would suggest that the duration of diabetes we have studied was too short to identify an eventual massive loss of neurons, already atrophic, from apoptosis. Our findings did not fulfil this prediction, but instead demonstrated a remarkable resistance of sensory neurons to loss despite their expression of caspase-3, a molecule often considered to be inexorably linked to apoptosis.

RESEARCH DESIGN AND METHODS

Animal preparation. Male Sprague-Dawley rats (weight 200–300 g at onset) were used for the experiment. Diabetes was induced by a single intraperitoneal injection of streptozotocin (STZ) (65 mg/kg). Controls received the STZ citrate buffer carrier alone. Additional control rats were noninjected male Sprague-Dawley rats weighing 200–300 g. The cohort of rats used in this study formed the basis of other previously reported investigations (5,20). The protocol was reviewed and approved by the University of Calgary Animal Care Committee based on the guidelines of the Canadian Council on Animal Care.

Rats were maintained on sawdust-covered plastic-bottomed cages and had access to rat water ad libitum. The whole blood glucose level was measured with a glucometer (AccuCheck; Boehringer Mannheim Canada, Dorval, Canada). Rats with a whole blood glucose level of ≥16.0 mmol/l were considered diabetic. Hyperglycemia was confirmed using fresh plasma and a glucose oxidase method (Ektachem DT6011 Analyzer; Kodak, Rochester, NY). In the same cohort of rats previously reported by our laboratory (5), there was slowing of motor and sensory conduction velocity, and diabetic rats weighed less than nondiabetic controls. One year later, diabetic and nondiabetic control rats were killed and tissue was harvested. L4 and L5 dorsal root ganglia (DRG) were rapidly removed during anesthesia (within ~30 min) for immunohistochemical and light and electron microscopic studies.

Immunohistochemistry and deconvolution imaging. Tissue samples were fixed in modified Zamboni's fixative (2% paraformaldehyde, 0.5% picric acid, and 0.1% phosphate buffer) overnight at 4°C. Tissues were then washed in PBS five times, cryo-protected in 20% sucrose/PBS, and left at 4°C overnight. After embedding in optimum cutting temperature (OCT) compound (Miles Laboratories, Elkart, IN), 16-μm thick sections were placed on poly-L-lysine–coated slides. For Bcl-2 immunohistochemical staining, samples were fast frozen, embedded in OCT, and stored at −80°C. Then 14-μm sections were placed on slides and postfixed with acetone at −20°C for 10 min.

Neurons and their process were labeled by monoclonal antineurofilament 200 antibody (1:800, Sigma). Macrophages were recognized by mouse monoclonal anti-ED-1 (1:1,000, Chemicon). The following apoptosis-related primary antibodies were used: rabbit antiprocaspase-3 and the cleaved p20 fragment caspase-3 polyclonal antibody (1:100, Chemicon), anticleaved caspase-3 rabbit polyclonal antibody (1:100, Trevigen), monoclonal mouse antibody recognizing poly(ADP-ribose) polymerase (PARP) (1:100, Trevigen), which recognizes both the full-length and cleaved molecule, polyclonal rabbit anti-rat/mouse Bcl-2 antibody (BD PharMingen), and mouse monoclonal anticytochrome c (1:50, Zymed Laboratories, San Francisco). Secondary antibodies were sheep anti-mouse IgG CY3 conjugate (1:100, Sigma) or Alexa Fluor 488 goat anti-rabbit IgG (H + L) conjugate (1:500, Cedarlane Laboratories, Hornby, ON, Canada).

For indirect immunofluorescence, slides were incubated for 48 h at 4°C with primary antibodies, washed with PBS, and incubated with secondary antibodies for 1 h at room temperature. After further PBS washing, coverslips were mounted with bicarbonate-buffered glycerol (pH 8.6), and slides were viewed with a fluorescent microscope (Axioskop; Zeiss).

Controls included omission of primary or secondary antibodies on parallel sections. DRG sections from young nondiabetic rats were also used as controls for detecting the normal pattern of some antibody labeling. A marker of nuclei, 4′,6-diamidino-2-phenylindole (DAPI), was used to counterstain DNA. After immunohistochemical labeling, Vectashield mounting medium with DAPI (Vector Laboratories, Burlington, ON) was used for mounting slides.

After immunofluorescent staining, digital sectioning (digital "confocal" microscopy) was performed for selected studies by using a Leica DM-RXA2 fluorescent microscope. Series images were taken by Princeton Instruments ST-138 with KAF 1660 cooled to −40°C, collected at 0.5- to 1.0-μm intervals. Stacks of images with slices at the same Z position (±0.05 μ) were collected for each fluorochrome. The deconvoluted images were obtained using Vaytek Microtome version 6.1 (Fairfield, IA). Images were converted to 8-bit red-green-blue (RGB) on false color. The deconvoluted images were rescaled to cover the entire 255-value gray range and further processed in Adobe Photoshop (25).

Apoptotic cell death detection (transferase-mediated dUTP nick-end labeling technology). Apoptotic cell death was detected by using an in situ cell death detection fluorescein kit (Roche Molecular Biochemicals) based on labeling of DNA strand breaks (transferase-mediated dUTP nick-end labeling [TUNEL] technology). L4 and L5 DRG from 1-year diabetic, 1-year control, and normal rats (n = 3 for each group) were removed, fast frozen, and immediately embedded in OCT compound in precooled 2-methylbutane in dry ice. Sections 14 μm thick were mounted on slides and postfixed in freshly made 4% paraformaldehyde in PBS for 20 min at room temperature. After washing for 30 min in PBS, slides were permeabilized in 0.1% Triton X-100/0.1% sodium citrate for 2 min on ice and then incubated in TUNEL reaction mixture at 37°C for 1 h. After TUNEL staining, slides were washed in PBS three times and covered. Each experiment included a negative and a positive control slide. For negative control, slides were incubated in the label solution only (without the terminal deoxynucleotidyl transferase). The positive control slides were treated with 3,000 units/ml DNase I for 10 min before incubating in the TUNEL reaction mixture. All slides were viewed with the fluorescent microscope.

Light and electron microscope. L4 and L5 DRG were taken from 1-year control and diabetic rats and fixed in 2.5% glutaraldehyde in 0.025 mol/l cacodylate buffer overnight. After washing in 0.15 mol/l cacodylate, samples were postfixed with 2% osmium tetroxide in 0.12 mol/l cacodylate, dehydrated in graded alcohols, and embedded in epon. Sections 1 μm thick were cut using an ultramicrotome, stained with toludine blue, and viewed by a light microscope (Axioskop; Zeiss). Light microscopy with blinded grading has been reported by our lab in this cohort before (5). For electron microscopy, 70-nm thick sections were placed on copper grids and stained with 10% uranyl and 0.1% lead citrate. The grids were examined with an H7000 transmission electron microscope (X2500-15000). Neurons were examined from the entirely randomly selected sections.

Counting caspase-3 and Bcl-2 profiles. For comparing the immunohistochemical staining of caspase-3 (procaspase-3 and the cleaved p20 fragment caspase-3), sections of L4 DRG from diabetic and control groups were postfixed and stained with this antibody. Six digital DRG images were taken randomly from each rat at the same magnification (400×). Caspase-3 immunoreactive profiles were counted and the mean calculated from six sections of each of three rats per group.

For counting the Bcl-2–positive neurons between diabetic and control groups, sections from L5 DRG of each rat were mounted on slides at 80-μm intervals. After immunohistochemical staining, Bcl-2 immunoreactive neurons were counted in sequential sections until 200 Bcl-2 immunoreactive neurons were reached. The percentage of Bcl-2 neurons out of total neuron profiles was then calculated (n = 3 for each group).

Analysis. Results were compared as means ± SE using two-tailed Student's t tests.

RESULTS

Diabetic cohort. As previously reported (5), diabetic rats weighed less than controls (415 ± 15 vs. 760 ± 16 g), had whole blood hyperglycemia (18.1 ± 0.6 vs. 4.9 ± 0.2 mmol/l), and had slowing motor (43.9 ± 0.9 vs. 52.5 ± 1.1 m/s) and sensory (54.9 ± 0.9 vs. 56.8 ± 0.7) conduction velocities (n = 26 diabetic and 27 nondiabetic rats in the cohort).

Caspase-3 expression in proximal axon segments and perikarya rises in diabetes. We applied two anti–caspase-3 antibody markers. The first was directed toward procaspase-3 (32 kDa) and the cleaved p20 fragment, and the second primary antibody exclusively recognized cleaved caspase-3 only. Discrete profiles labeled with the procaspase/p20 antibody were detected in proximal axon segments of neurons (Fig. 1*A* and *B*), which was confirmed by double labeling in transverse and longitudinal sections with NF200 antibody directed against the heavy neurofilament subunit [Fig. 1*C*, *C*(*a*), and *C*(*b*)]. This caspase-3 antibody generally did not label perikarya. There was a

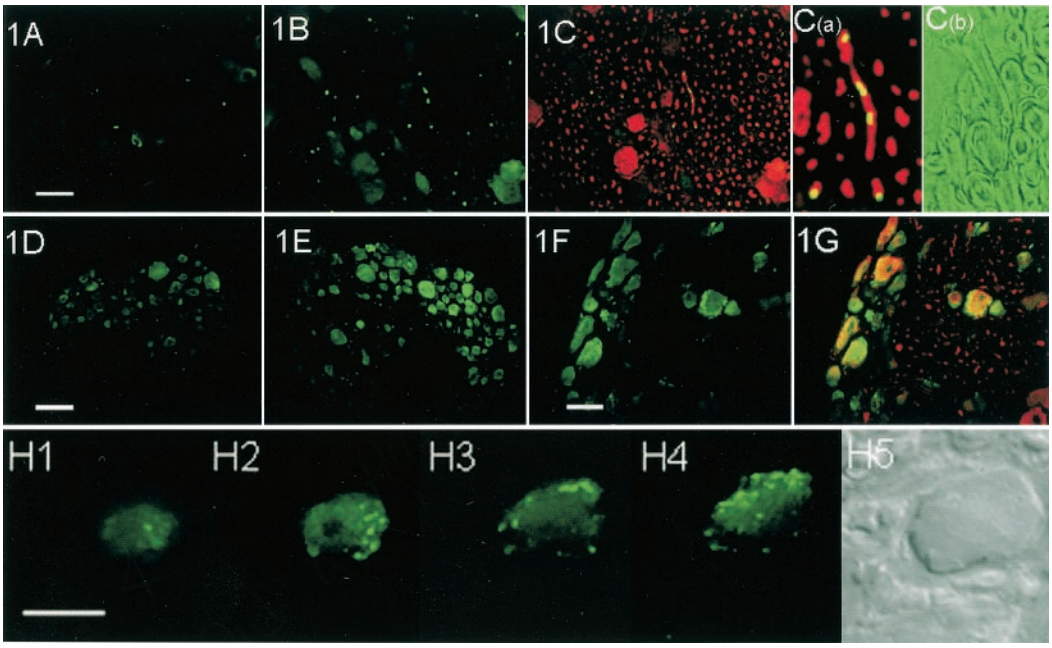

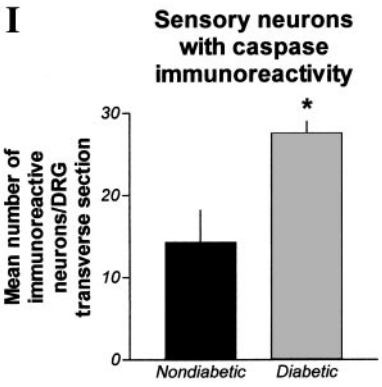

FIG. 1. Caspase-3 is activated and increased in 1-year experimental diabetic DRG neurons. *A–C*: Antipro and cleaved caspase-3 immunohistochemical staining in 1-year control and 1-year diabetic DRG. *A*: Nondiabetic DRG showed discrete immunoreactive profiles in nonneuronal areas, whereas neuron perikarya were largely unlabeled. *B*: Diabetic DRG had a similar pattern of immunoreactivity, but there were more caspase-3 profiles. *C*: The same field as *B*, double labeled for neurofilament (red), illustrating that pro- and cleaved caspase-3 were present in proximal axon segments. *C*(*a*): Enlarged image from *C*. Diabetic caspase-3 profiles lined up in axons that were double labeled with NF 200 in longitudinal and cross-sectioned fibers. *C*(*b*): Transmitted light image taken from the same field as *C*(*a*), confirming that caspase-3 was located in the axons of myelinated fibers. *D–G*: Anti-cleaved caspase-3 immunohistochemical staining in 1-year control and diabetic DRG. In nondiabetic DRG (*D*), only occasional neurons had caspase-3 immunoreactivity, whereas in diabetic DRG (*E*) there were greater numbers of labeled neurons. Higher magnification images in diabetic DRG labeled with caspase-3 (*F*), illustrating double labeling with neurofilament (*G*). Cleaved caspase-3 was present in sensory neuron cytoplasm and nuclei. *H1–4*: Optical sectioning and digital deconvolution of diabetic sensory neurons, demonstrating the distribution of cleaved cytoplasmic caspase-3. *H1–4* represent the serial section of a neuron with an interval of 2 μm. *H5:* Transmitted light image of the same field. *I*: Quantitation of caspase-3 labeled neurons. **P* ≤ 0.05. Bar = 50 μm in *A–C*, *F*, and *G*; 100 μm in *D* and *E*; and 7.4 μm in *H*.

significant increase in labeled profiles observed in diabetic animals compared with the nondiabetic control group (Fig. 1).

Labeling with an antibody to cleaved caspase-3 antibody also confirmed that there were rises in diabetic neurons with immunoreactivity in proximal axon segments, as above, but also within perikarya. The latter labeling, only very rarely observed in nondiabetic control neurons, was diffuse cytoplasmic, multifocal cytoplasmic, and occasionally nuclear (Fig. 1*D–H*). Occasional satellite cells in both nondiabetic (in both young control rats and citrate-injected nondiabetic rats at 12 months) and diabetic DRG were labeled with the antibody to cleaved caspase-3. Sural nerves had no evidence of caspase-3 immunoreactivity using either antibody approach.

Rises in PARP expression. In nondiabetic DRG, PARP immunohistochemical labeling was largely confined to neuron nuclei. Similar findings were encountered whether young nondiabetic rat DRG were examined or the 12-month nondiabetic control group. Small PARP profiles outlined most neuron nuclei, which was confirmed by double labeling with the nuclear marker DAPI (Fig. 2*A–B*). PARP expression differed in diabetic neurons, (Fig. 2*C–D*) with somewhat more prominent labeling of neuronal nuclei and cytoplasm, and also in proximal axons, seen using serial optical imaging (Fig. 2*E*). Some PARP immunoreactivity was also observed in the nuclei of the satellite cells (Fig. 2*E*), a pattern not observed in nondiabetic controls. PARP immunoreactivity did not generally colocalize with that of caspase-3.

Sensory neurons are not labeled by TUNEL in diabetes and do not have apoptotic nuclear morphology. Assuming that the activation of caspase-3 was inexorably linked to genomic DNA fragmentation, we applied TUNEL to sections of diabetic and nondiabetic DRG. Each series of labeled slides included a positive control using DNase I to fragment DNA and a negative control slide to eliminate terminal deoxynucleotidyl transferase. In positive control slides, numerous TUNEL-positive cells included satellite cells, Schwann cells, DRG capsule cells, and a few neurons (Fig. 3*A* and *B*). Slides were counter stained with toludine blue to confirm the identity of the labeled cells (Fig. 3*B*). Negative control slides did not have TUNEL, as expected.

In ganglia of long-term diabetic and nondiabetic rats, only occasional satellite cells were TUNEL positive (Fig.

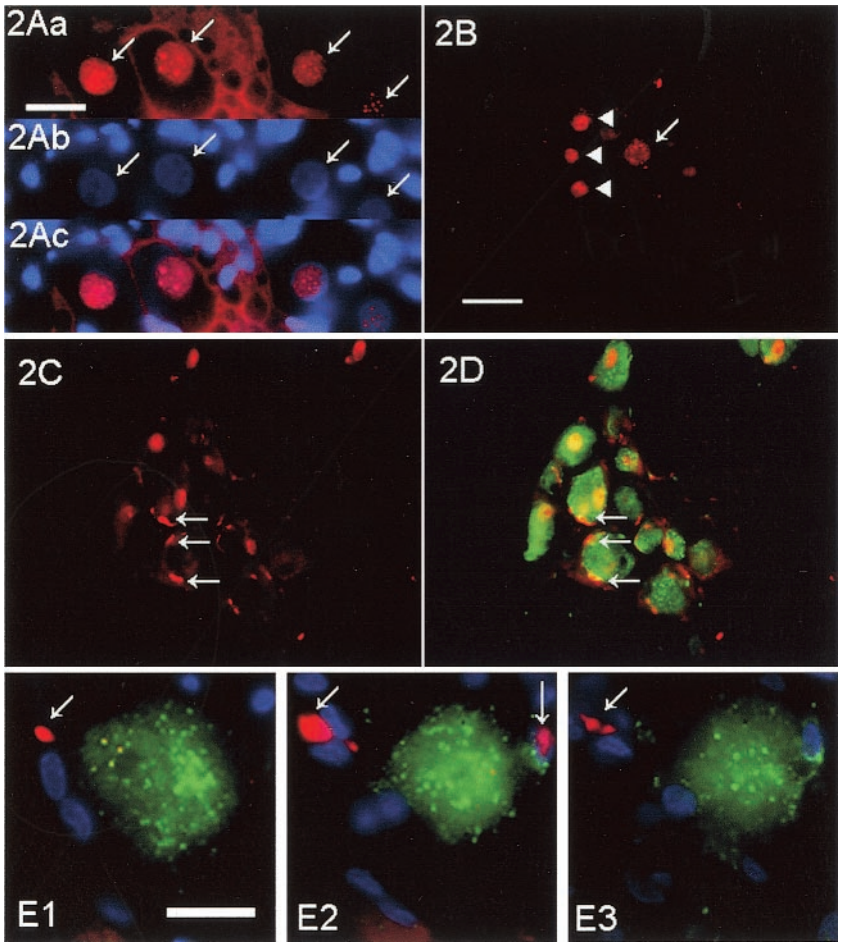

FIG. 2. PARP expression is increased and altered in 1-year experimental diabetic DRG neurons. *A*: Anti-PARP immunohistochemical staining in young nondiabetic control DRG. *Aa*: Four neuronal nuclei have PARP labeling (arrows). *Ab*: Same field as *Aa*, counterstained with DAPI, outlines nuclei in four neurons (arrows) and also satellite cells surrounding neurons. *Ac*: Double-labeled image indicating PARP localization in neuronal nuclei. *B*: PARP in 1-year nondiabetic DRG. Three neurons have PARP immunoreactivity (arrowheads), whereas another neuron speckled with PARP immunoreactivity was in the cytoplasm of a neuron (arrow). *C*: PARP in 1-year diabetic DRG. PARP was found not only in neuronal nuclei, but also in proximal axon segments (*E*) surrounding neurons (arrows). *D*: Same image as *C*, double labeled with PARP and cleaved caspase-3 antibodies, illustrating PARP not only in neuronal nuclei but also in surrounding neurons (arrows). *E1-3*: Optical sections of a diabetic sensory neuron with an interval of 8 μm. A PARP immunoreactive profile (red) in the left upper corner of each panel represents a proximal axon segment because it is not double labeled with the DAPI nuclear marker (blue) or activated caspase-3 (green). The DAPI labeled profile (in *E2* [right upper corner]) was a satellite cell nucleus. Bar = 20 μm in *A*; 50 μm in *B–D*; and 16 μm in *E*.

3*D*). Neurons were not labeled. In addition to TUNEL staining, we examined the pattern of DAPI staining of ganglia cell populations. No characteristic nuclear clumping or fragmentation expected of apoptosis was observed in neurons (Fig. 3*E–H*).

Features of apoptosis are not detected by electron microscopy. Random sampling of thin electron microscopy sections was made and included a minimum of 60–80 neurons in each of three rats from both the nondiabetic and diabetic groups. None of the neuronal nuclei had chromatin condensation or fragmentation to suggest apoptosis, and cytoplasmic blebbing associated with neurons or in other fields was not observed (Fig. 4). There was an apparent increase in lipofuscin pigment in diabetic neurons.

Bcl-2 and cytochrome c expression is unchanged in diabetic neurons. To evaluate an antiapoptosis signaling factor that could contribute to neuron survival in diabetes, we labeled ganglia with an antibody directed against Bcl-2, a member of the antiapoptotic cascade. Bcl-2 immunohistochemical staining was largely confined to the cytoplasm of small-diameter sensory DRG neurons in both diabetic and nondiabetic control neurons (Fig. 5). There was no difference in the proportion of Bcl-2–labeled neurons between nondiabetic control and diabetic ganglia (Fig. 5*G*). Discrete Bcl-2 labeling was also observed in axons and blood vessels without detectable differences between diabetic and control subjects. Cytochrome c neuronal labeling appeared confined to discrete profiles most likely representing cytoplasmic mitochondria (data not shown). There was no apparent difference between diabetic and control subjects and otherwise no evidence of cytochrome c presence in the cytosol.

Nitrotyrosine expression and macrophages in 1-year control and diabetic DRG. In DRG harvested from young rats, rare nitrotyrosine-labeled profiles were observed in the cytoplasm of Schwann cells (data not shown). In 1-year diabetic and nondiabetic control groups, nitrotyrosine antibody also labeled the cytoplasm of occasional small neurons and occasional proximal axon segments (Fig. 6). Nitrotyrosine immunoreactivity appeared more prevalent in diabetic neurons, but labeling was judged not sufficiently discrete to permit specific counting. Rare ED-1–labeled macrophage profiles were observed in both diabetic and nondiabetic DRG without a difference between the groups.

DISCUSSION

The major findings of this study are as follows. First, DRG sensory neurons in a model of long-term experimental diabetes (12 months) failed to exhibit any features of apoptosis, such as nuclear fragmentation, clumping on DAPI staining or electron microscopy, or TUNEL. Second, while apoptosis did not occur in diabetic sensory neurons, there was heightened expression of activated caspase-3 in nuclei, cytoplasm, and proximal axon segments. Third, PARP labeling was enhanced in diabetic neurons and was

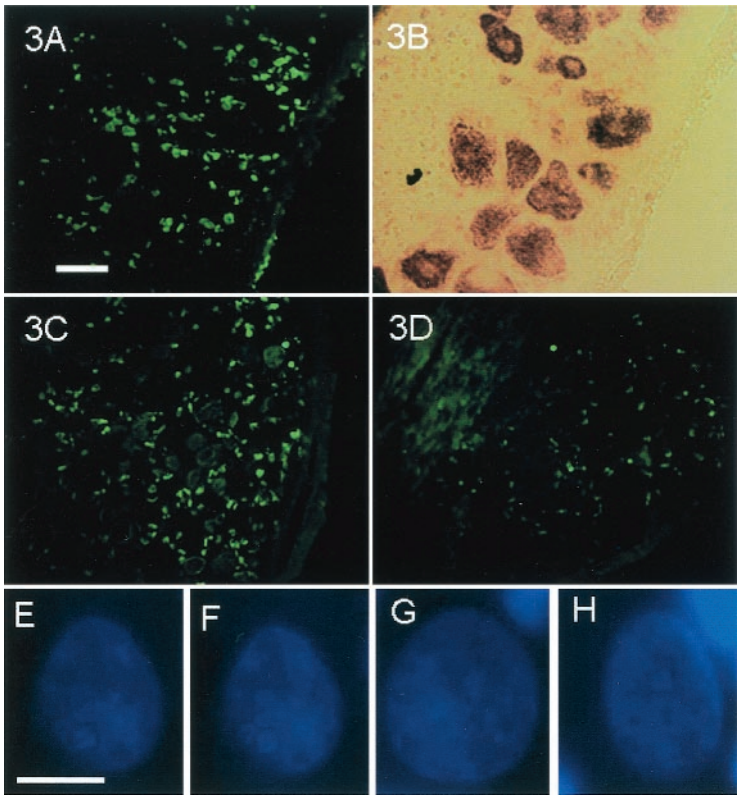

FIG. 3. TUNEL and DAPI staining do not show chromatin degradation or nuclear fragmentation in 1-year diabetic DRG neurons. *A*: Positive control of TUNEL, generated by applying DNase to the section, from a 1-year nondiabetic DRG. The labeled nuclei are largely from satellite cells and DRG capsule cells but not neurons. *B*: Same field as *A* under light microscopy and counterstained with toluidine blue to confirm cellular identity. *C*: Positive control using DNase and TUNEL from 1-year diabetic DRG with labeled satellite and capsule cells. Occasionally neuronal nuclei were labeled. *D*: TUNEL of untreated 1-year diabetic DRG. Only occasional satellite cells, but not neurons, were labeled. *E–H*: Representative images of DAPI staining in sensory neuronal nuclei of 1-year diabetic DRG. There was no characteristic nuclear fragmentation of those neurons. Bar = 50 μm in *A–D* and 10 μm in *E–H*.

expressed in nuclei, cytoplasm, and proximal axon segments. Fourth, Bcl-2 expression was neither upregulated nor downregulated in experimental diabetes. Finally, nitrotyrosine is expressed in DRG neurons of diabetic and nondiabetic rats of older age with a trend toward greater labeling in diabetic subjects. Macrophage infiltration was not increased in diabetes.

The above evidence needs to be coupled with our findings reported previously in the same model (5), indicating that: *1*) unbiased physical counts of the entire L5 DRG did not identify neuron dropout; *2*) downstream sural axons were preserved in number (chronic cumulative neuron dropout over 12 months should have been easily detectable by either method); and *3*) blinded assessment of 100–150 neurons under light microscopy in each of five diabetic and five nondiabetic rats did not identify significant evidence of degeneration, loss (nests of Nageotte), or apoptosis accompanying diabetes.

Several approaches are available to evaluate possible activation of the death-inducing signaling cascades in diabetes. Upstream activators include Fas/tumor necrosis factor-α, which recruits procaspases through the death-inducing signaling complex, eventually activating effector caspases 3, 6, and 7 (26). As postulated in diabetes, activation of death pathways may instead be more likely to occur through mitochondrial pore formation (27). The latter step in turn releases cytochrome c and, with Apaf-1 and caspase-9, forms the apoptosome, which then generates a downstream cascade of caspase activation. Other putative players in this complex pathway not addressed in the present study are upstream members of the caspase family, Jun NH_2-terminal kinase, nuclear factor κ-B, phosphatidylinositol 3-kinase/Akt, second mitochondria-derived activator of caspase/DIABLO, and others (27,28). In this study, we selected several key steps putatively linked to diabetic neurons by previous studies: caspase-3 proenzyme and its activated product as critical downstream activators of cell death; Bcl-2, an inhibitor of mitochondrial pore formation; and PARP, a target of caspase cleavage and also a repair enzyme.

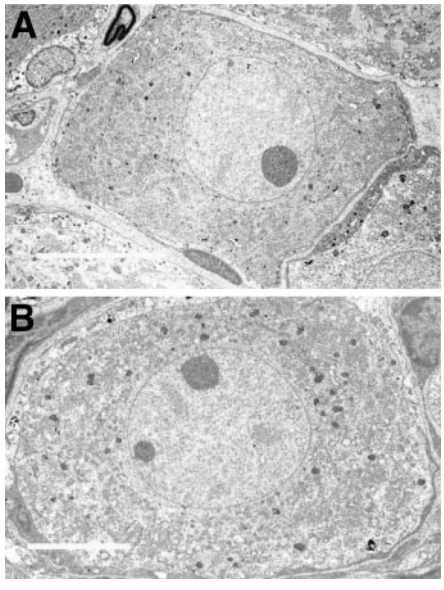

FIG. 4. Electron microscopic images do not show typical characteristics of neuronal apoptosis. *A*: Representative electron microscopy image of a 1-year nondiabetic DRG neuron. *B*: Representative electron microscopy image of a 1-year diabetic DRG neuron. There were no apoptotic changes, such as chromatin margination and nuclear condensation, in any of the neurons examined. Bar = 10 μm.

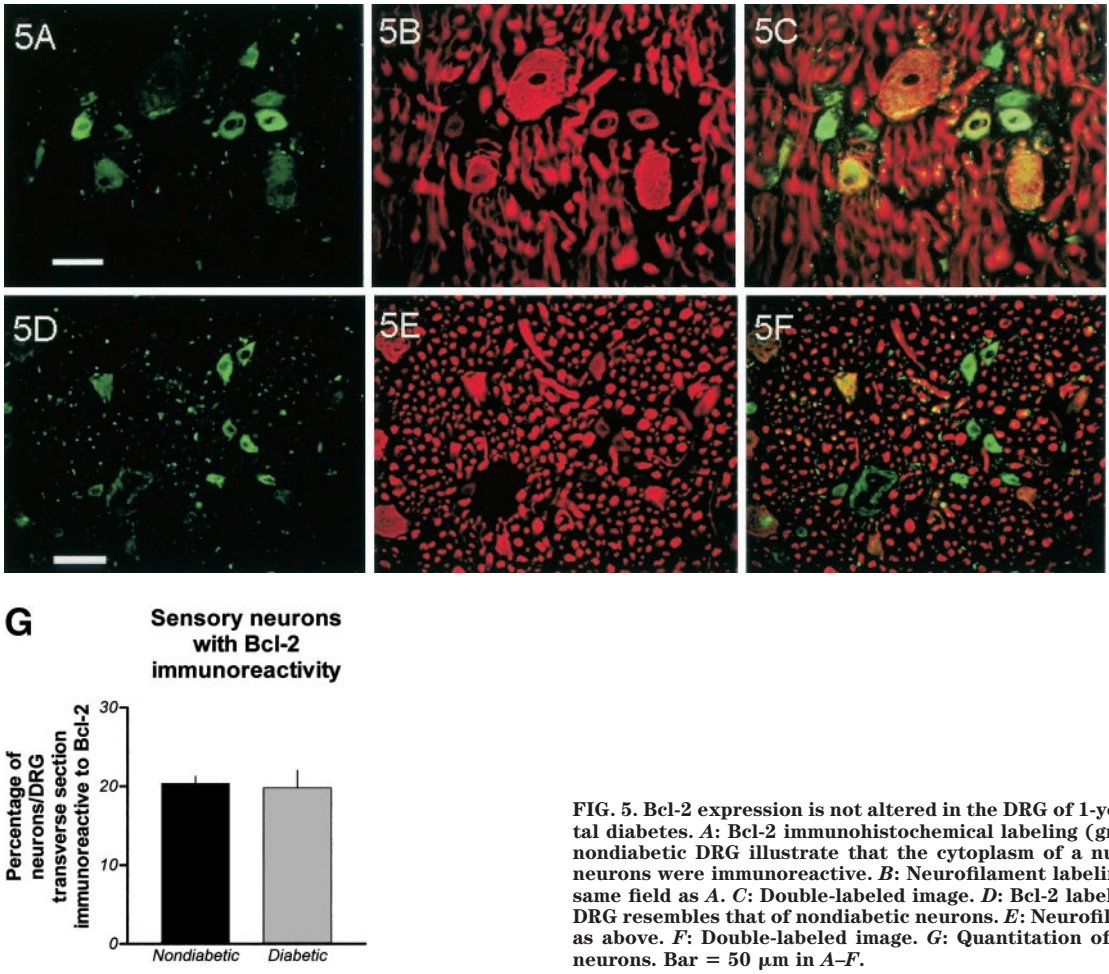

FIG. 5. Bcl-2 expression is not altered in the DRG of 1-year experimental diabetes. *A*: Bcl-2 immunohistochemical labeling (green) in 1-year nondiabetic DRG illustrate that the cytoplasm of a number of small neurons were immunoreactive. *B*: Neurofilament labeling (red) of the same field as *A*. *C*: Double-labeled image. *D*: Bcl-2 labeling in diabetic DRG resembles that of nondiabetic neurons. *E*: Neurofilament labeling as above. *F*: Double-labeled image. *G*: Quantitation of Bc1-2–labeled neurons. Bar = 50 μm in *A*–*F*.

We applied particular rigor to addressing the thorny question of whether apoptosis was actually ongoing by combining unbiased physical dissector counting (not done before in the models), morphological changes under the light and electron microscope, and three potential assays of apoptosis. An immunohistochemical approach was required for all of the players examined in this study because immunoblots or other approaches would not provide information about selective protein expression in neurons alone. Abnormal vacuolation of sensory neurons has been considered an index of apoptosis-related mitochondrial dysfunction in diabetes in some studies (29). While mitochondrial dysfunction may be a key element of cellular damage in diabetes, microvacuolar change as observed

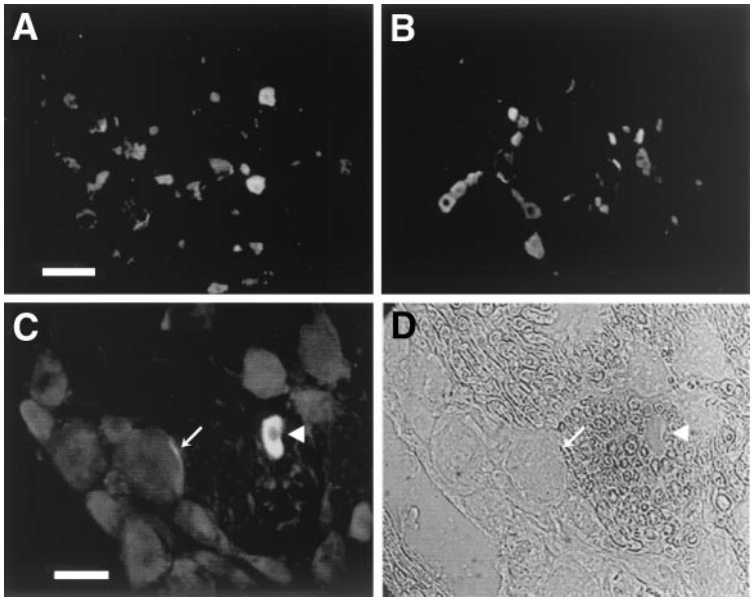

FIG. 6. Nitrotyrosine expression is more prominent in DRG of 1-year experimental diabetes. *A*: Nitrotyrosine immunohistochemical labeling in 1-year nondiabetic DRG. Occasional small neurons were labeled. *B*: Diabetic DRG suggested greater neuronal labeling in addition to profiles surrounding and between neurons. *C*: Diabetic DRG under higher power magnification shows a labeled neuron (arrowhead) and a proximal axon segment (arrow). *D*: Same field as *C* with transmitted light. Bar = 100 μm in *A* and *B* and 50 μm in *C* and *D*.

under light microscopy has been nonselective and can occur as a function of postmortem harvesting (X.-Q. Li and D.W.Z., unpublished observations).

We identified procaspase-3 and the p20 cleaved fragment labeling to be largely in axons, whereas activated caspase-3 was also observed in neuronal soma and nuclei. The presence of limited staining in nondiabetic control ganglia axons and cytoplasm may reflect low-level constitutive expression of the proenzyme. In diabetes there was more widespread expression, which was also in nuclei, unlike controls. Mechanisms postulated to account for heightened activation of caspase-3 in diabetes include oxidative and nitrative stress, growth factor deficiency, ischemia, and perhaps excessive polyol flux (8,16,19,21, 22,30–34). In our model, activated caspase-3 was not detectable in sural axons. The overall pattern is different from an apparent retrograde activation of caspase-3 after target removal in olfactory neurons reported by Cowan et al. (35).

The findings indicate that sensory neurons are directly vulnerable to diabetic damage. Despite heightened caspase-3 activation, we provide convincing evidence against ongoing apoptosis. Cell shrinkage, aggregation of chromatin at the nuclear membrane, and formation of membrane blebbing was not observed under light and electron microscopy. Furthermore, unbiased physical dissection counts of the entire L5 DRG did not identify significant neuron loss in the same cohort of rats. Is it possible that apoptosis occurs too rapidly to be detected in neurons at a given time point, particularly if only a smaller proportion of neurons are dying at any given time? Any significant form of ongoing loss, however, should have led to a reduction of counted neurons, but it did not.

It has been widely accepted that the activation of effector caspases, such as caspase-3, will eventually lead to apoptosis of a cell. This view, however, has recently been challenged (36). In some instances, the activation of caspase-3 does not commit a cell to apoptosis. The balance of pro- and antiapoptotic cascades and their interaction with adjacent supporting cells is complex. Reddien et al. (37) reported that in *C. elegans*, cells expressing CED-3 caspase—the homologue of mammalian caspase-3—survive and even differentiate, passing through a stage called "mostly dead," which resembles the early phase of apoptosis (38). Hinck et al. (39) noted that hyperglycemia induced caspase-mediated nuclear chromatin degradation but that high glucose–induced nuclear fragmentation was not linked to caspases. Here we provide new evidence that caspase-3 activation is not always fatal in vertebrates.

TUNEL may reflect chronic mild DNA injury in some models that is repaired by enzymes such as PARP. A more recent report (40) suggested the presence of caspase activation and extensive apoptosis in a model of experimental diabetes lasting 12 months. In this study the number of DRG neurons expressing caspase-3 was also increased at earlier time points. TUNEL cells, which are increased in diabetes, were used to identify apoptosis. In our study we argue, as have others, that morphological criteria of neurons undergoing apoptosis, unequivocal cell and axon loss, and replacement of neurons by nests of Nageatte are critical in proving that apoptosis exists. Regardless of these differences, our studies do support the concept that apoptotic actors are activated by diabetic stress. A further report examining intact neurons in STZ-induced diabetes only identified TUNEL-positive DRG sensory neurons after axon injury (41). Apoptotic cell death was not observed in sensory neurons of mouse spinal ganglia (42).

PARP is a substrate of both caspase-3 activation in apoptosis and an enzyme activated by peroxynitrite. Its nuclear localization in nondiabetic ganglia is an expected feature of its function in repairing DNA injury. In diabetes, however, PARP had heightened not only cytoplasmic localization but also movement out into proximal axon segments. We also identified novel PARP expression in diabetic perineuronal satellite cells. There is evidence that this population may provide critical support for neurons, and it is also possible that satellite cells retain their supportive role for neurons by proliferating when they are directly targeted. The axonal localization of PARP may reflect activation of mechanisms to repair damaged mitochondrial DNA, a postulated mechanism of cell death in diabetic neurons (24,43,44). Our antibody did not distinguish whether increased PARP in diabetes was from the parent molecule or cleaved product.

Nagayama et al. (45) reported that after sublethal transient global ischemia, activation of PARP in rat hippocampus might contribute to cellular recovery. The cleavage of PARP by caspases (such as caspase-3) facilitates cellular disassembly and serves as a marker of cells undergoing apoptosis. In other conditions, such as exposure to peroxynitrite and saturating levels of DNA damage, excessive PARP activity has been thought to lead to cell death through unregulated consumption of high-energy metabolites by the enzyme (46,47).

Chronic low-grade rises in peroxynitrite elaboration, and perhaps toxicity, may occur in diabetic ganglia. In a previous study, we found evidence that long-term (12 months) diabetic ganglia had increased activity of nitric oxide synthase, thus likely generating local rises in nitric oxide content (20). The reaction of nitric oxide with superoxide forms the toxic metabolite peroxynitrite, whose footprints in turn appear as nitrotyrosine immunoreactivity. Endocardial biopsies from diabetic patients identified both nitrotyrosine labeling and apoptosis (48).

Another unexpected finding in our study was the absence of alterations in Bcl-2 intensity in diabetes. When cells are exposed to stimuli that trigger apoptosis, cytochrome c is released from mitochondria into cytoplasm, where it activates caspases. By preventing the release of cytochrome c, Bcl-2 protein interferes with this activation of caspases and prolongs cell survival. Srinivasan et al. (24) reported decreased Bcl-2 in 3- to 6-week diabetic DRG, suggesting increased risk for apoptosis. We found no such change, which further supports arguments against active apoptosis occurring in our population and evidence that other "repair" cascades may be involved in protecting diabetic sensory neurons. Also, since Bcl-2 appeared to be mainly concentrated in small-diameter neurons, whereas caspase-3 distribution was more widespread, other factors are also likely to protect neurons from apoptosis. One of the candidates might be HSP-27 (heat shock protein 27, a survival protein), which was found to have elevated mRNA

levels in DRG neurons in our previous report of this model (5,49).

In summary, diabetic stress triggers molecular actors in the apoptotic pathway, but unique defense mechanisms likely protect long-term diabetic sensory neurons from apoptosis. Understanding and exploiting such mechanisms may offer new avenues in the treatment of human diabetic polyneuropathy.

ACKNOWLEDGMENTS

This study was supported by an operating grant from the Canadian Institutes of Health Research. D.W.Z. is a Senior Medical Scholar of the Alberta Heritage Foundation for Medical Research.

Brenda Boake provided expert secretarial assistance. Dr. W.M. Schoel, W-X. Dong, and R.W. Humphrey of the University of Calgary Microscopy and Imaging Facility kindly assisted with deconvolution and electron microscopy.

REFERENCES

1. Zochodne DW: Is early diabetic neuropathy a disorder of the dorsal root ganglion? A hypothesis and critique of some current ideas on the etiology of diabetic neuropathy. *J Peripher Nerv Syst* 1:119–130, 1996
2. Zochodne DW, Ho LT: Unique microvascular characteristics of the dorsal root ganglion in the rat. *Brain Res* 559:89–93, 1991
3. Arvidson B: Distribution of protein tracers in peripheral ganglia: a light and electron microscopic study in rodents after various modes of tracer administration. *Acta Univ Ups* 344:1–72, 1979
4. Scott JN, Clark AW, Zochodne DW: Neurofilament and tubulin gene expression in progressive experimental diabetes: failure of synthesis and export by sensory neurons. *Brain* 122:2109–2117, 1999
5. Zochodne DW, Verge VMK, Cheng C, Sun H, Johnston J: Does diabetes target ganglion neurons? Progressive sensory neuron involvement in long term experimental diabetes. *Brain* 124:2319–2334, 2001
6. Borghini I, Ania-Lahuerta A, Regazzi R, Ferrari G, Gjinovci A, Wollheim CB, Pralong WF: Alpha, beta I, beta II, delta, and epsilon protein kinase C isoforms and compound activity in the sciatic nerve of normal and diabetic rats. *J Neurochem* 62:686–696, 1994
7. Brett FM, Kalichman MW, Calcutt NA, Mizisin AP: Effects of seven days of galactose feeding and aldose reductase inhibition on mast cells and vessel morphometry in rat sciatic nerve. *J Neurol Sci* 141:6–12, 1996
8. Greene DA, Lattimer SA, Sima AA: Sorbitol, phosphoinositides, and sodium-potassium-ATPase in the pathogenesis of diabetic complications. *N Engl J Med* 316:599–606, 1987
9. Gupta S, Sussman I, McArthur CS, Tornheim K, Cohen RA, Ruderman NB: Endothelium-dependent inhibition of Na(+)-K+ ATPase activity in rabbit aorta by hyperglycemia: possible role of endothelium-derived nitric oxide. *J Clin Invest* 90:727–732, 1992
10. Mizisin AP, Li L, Calcutt NA: Sorbitol accumulation and transmembrane efflux in osmotically stressed JS1 schwannoma cells. *Neurosci Lett* 229: 53–56, 1997
11. Sima AAF, Brismar T, Yagihashi S: Neuropathies encountered in the spontaneously diabetic BB Wistar rat. In *Diabetic Neuropathy.* Dyck PJ, Thomas PK, Asbury AK, Winegrad AI, Porte D Jr, Eds. Toronto, W.B. Saunders, 1987, p. 253–259
12. Roberts RE, McLean WG: Protein kinase C isozyme expression in sciatic nerves and spinal cords of experimentally diabetic rats. *Brain Res* 754:147–156, 1997
13. Tuck RR, Schmelzer JD, Low PA: Endoneurial blood flow and oxygen tension in the sciatic nerves of rats with experimental diabetic neuropathy. *Brain* 107:935–950, 1984
14. Zochodne DW, Ho LT: The influence of indomethacin and guanethidine on experimental streptozotocin diabetic neuropathy. *Can J Neurol Sci* 19: 433–441, 1992
15. Zochodne DW, Ho LT: Normal blood flow but lower oxygen tension in diabetes of young rats: microenvironment and the influence of sympathectomy. *Can J Physiol Pharmacol* 70:651–659, 1992
16. Low PA, Nickander KK, Tritschler HJ: The roles of oxidative stress and antioxidant treatment in experimental diabetic neuropathy. *Diabetes* 46 (Suppl. 2):S38–S42, 1997
17. Ceriello A, Giugliano D: Oxidative stress and diabetic complications. In *International Textbook of Diabetes Mellitus.* Alberti KGGM, Zimmet P, DeFronzo RA, Keen HH, Eds. Chichester, NY, John Wiley & Sons, 1997, p.1453–1461
18. Ryle C, Donaghy M: Non-enzymatic glycation of peripheral nerve proteins in human diabetics. *J Neurol Sci* 129:62–68, 1995
19. Brewster WJ, Fernyhough P, Diemel LT, Mohiuddin L, Tomlinson DR: Diabetic neuropathy, nerve growth factor and other neurotrophic factors. *Trends Neurosci* 17:321–325, 1994
20. Zochodne DW, Verge VM, Cheng C, Hoke A, Jolley C, Thomsen K, Rubin I, Lauritzen M: Nitric oxide synthase activity and expression in experimental diabetic neuropathy. *J Neuropathol Exp Neurol* 59:798–807, 2000
21. Zochodne DW, Ho LT: The influence of sulindac on experimental streptozotocin-induced diabetic neuropathy. *Can J Neurol Sci* 21:194–202, 1994
22. Zochodne DW, Ho LT, Allison JA: Dorsal root ganglia microenvironment of female BB Wistar diabetic rats with mild neuropathy. *J Neurol Sci* 127:36–42, 1994
23. Russell JW, Sullivan KA, Windebank AJ, Herrmann DN, Feldman EL: Neurons undergo apoptosis in animal and cell culture models of diabetes. *Neurobiol Dis* 6:347–363, 1999
24. Srinivasan S, Stevens M, Wiley JW: Diabetic peripheral neuropathy: evidence for apoptosis and associated mitochondrial dysfunction. *Diabetes* 49:1932–1938, 2000
25. Ou Y, Rattner JB: A subset of centrosomal proteins are arranged in a tubular conformation that is reproduced during centrosome duplication. *Cell Motil Cytoskeleton* 47:13–24, 2000
26. Tolkovsky A: Apoptosis in diabetic neuropathy. In *Neurobiology of Diabetic Neuropathy.* Tomlinson D, Ed. San Diego, Academic Press, 2002, p.145–159
27. Hirsch T, Susin SA, Marzo I, Marchetti P, Zamzami N, Kroemer G: Mitochondrial permeability transition in apoptosis and necrosis. *Cell Biol Toxicol* 14:141–145, 1998
28. MacManus JP, Buchan AM: Apoptosis after experimental stroke: fact or fashion? *J Neurotrauma* 17:899–914, 2000
29. Sasaki H, Schmelzer JD, Zollman PJ, Low PA: Neuropathology and blood flow of nerve, spinal roots and dorsal root ganglia in longstanding diabetic rats. *Acta Neuropathol* 93:118–128, 1997
30. Lyons TJ, Jenkins AJ: Glycation, oxidation, and lipoxidation in the development of the complications of diabetes: a carbonyl stress hypothesis. *Diabetes Rev* 5:365–391, 1997
31. Zochodne DW, Levy D, Zwiers H, Sun H, Rubin I, Cheng C, Lauritzen M: Evidence for nitric oxide and nitric oxide synthase activity in proximal stumps of transected peripheral nerves. *Neuroscience* 91:1515–1527, 1999
32. Greene DA, Sima AA, Stevens MJ, Feldman EL, Killen PD, Henry DN, Thomas T, Dananberg J, Lattimer SA: Aldose reductase inhibitors: an approach to the treatment of diabetic nerve damage. *Diabetes Metab Rev* 9:189–217, 1993
33. Greene DA, Sima AA, Stevens MJ, Feldman EL, Lattimer SA: Complications: neuropathy, pathogenetic considerations. *Diabetes Care* 15:1902–1925, 1992
34. Ishii H, Jirousek MR, Koya D, Takagi C, Xia P, Clermont A, Bursell SE, Kern TS, Ballas LM, Heath WF, Stramm LE, Feener EP, King GL: Amelioration of vascular dysfunctions in diabetic rats by an oral PKC beta inhibitor. *Science* 272:728–731, 1996
35. Cowan CM, Thai J, Krajewski S, Reed JC, Nicholson DW, Kaufmann SH, Roskams AJ: Caspases 3 and 9 send a pro-apoptotic signal from synapse to cell body in olfactory receptor neurons. *J Neurosci* 21:7099–7109, 2001
36. Hoeppner DJ, Hengartner MO, Schnabel R: Engulfment genes cooperate with ced-3 to promote cell death in *Caenorhabditis elegans*. *Nature* 412:202–206, 2001
37. Reddien PW, Cameron S, Horvitz HR: Phagocytosis promotes programmed cell death in *C. elegans*. *Nature* 412:198–202, 2001
38. Green DR, Beere HM: Apoptosis: mostly dead. *Nature* 412:133–135, 2001
39. Hinck L, Van Der Smissen P, Heusterpreute M, Donnay I, De Hertogh R, Pampfer S: Identification of caspase-3 and caspase-activated deoxyribonuclease in rat blastocysts and their implication in the induction of chromatin degradation (but not nuclear fragmentation) by high glucose. *Biol Reprod* 64:555–562, 2001
40. Schmeichel AM, Schmelzer JD, Low PA: Oxidative injury and apoptosis of dorsal root ganglion neurons in chronic experimental diabetic neuropathy. *Diabetes* 52:165–171, 2003
41. Kogawa S, Yasuda H, Terada M, Maeda K, Kikkawa R: Apoptosis and impaired axonal regeneration of sensory neurons after nerve crush in diabetic rats. *Neuroreport* 11:663–667, 2000
42. Sango K, Horie H, Saito H, Ajiki K, Tokashiki A, Takeshita K, Ishigatsubo Y, Kawano H, Ishikawa Y: Diabetes is not a potent inducer of neuronal cell

death in mouse sensory ganglia, but it enhances neurite regeneration in vitro. *Life Sci* 71:2351–2368, 2002
43. Schapira AH: Mitochondrial dysfunction in neurodegenerative disorders. *Biochim Biophys Acta* 1366:225–233, 1998
44. Mathews CE, Berdanier CD: Noninsulin-dependent diabetes mellitus as a mitochondrial genomic disease. *Proc Soc Exp Biol Med* 219:97–108, 1998
45. Nagayama T, Simon RP, Chen D, Henshall DC, Pei W, Stetler RA, Chen J: Activation of poly(ADP-ribose) polymerase in the rat hippocampus may contribute to cellular recovery following sublethal transient global ischemia. *J Neurochem* 74:1636–1645, 2000
46. Zhang J, Snyder SH: Nitric oxide and poly(ADP-ribose) polymerase in neuronal cell death. In *Cell Death: The Role of PARP*. Szabo C, Ed. CRC Press, Boca Raton, FL, 2000, p.7–22
47. Liu J, Ying W, Massa S, Duriez PJ, Swanson RA, Poirier GG, Sharp FR: Effects of transient global ischemia and kainate on poly(ADP-ribose) polymerase (PARP) gene expression and proteolytic clevage in gerbil and rat brains. *Mol Brain Res* 80:7–16, 2000
48. Frustaci A, Kajstura J, Chimenti C, Jakoniuk I, Leri A, Maseri A, Nadal-Ginard B, Anversa P: Myocardial cell death in human diabetes. *Circ Res* 87:1123–1132, 2000
49. Lewis SE, Mannion RJ, White FA, Coggeshall RE, Beggs S, Costigan M, Martin JL, Dillmann WH, Woolf CJ: A role for HSP27 in sensory neuron survival. *J Neurosci* 19:8945–8953, 1999